communications earth & environment

Article

A Nature Portfolio journal

https://doi.org/10.1038/s43247-025-02251-y

Arctic fjord ecosystem adaptation to cryosphere meltdown over the past 14,000 years

Jochen Knies[1,2] ✉, Youngkyu Ahn[3], Berenice Ebner[4], Lukas Smik[5,6], Kwangchul Jang[3,7], Seung-Il Nam[3], Simon T. Belt[6] & Carsten J. Schubert[8]

The Arctic cryosphere is the epicentre of acute global change impact, with abrupt warming and amplification driving rapid sea ice decline and irreversible glacial ice loss. A key challenge is understanding how the cryosphere meltdown will impact Arctic marine carbon cycles and ecosystems. Here, we use organic geochemical biomarkers to trace the contribution of different planktonic groups to organic carbon in Arctic fjord sediments (Kongsfjorden, Svalbard) during past warmer and colder (than present) climate states. We show that phytoplankton community structures changed abruptly with variable sea ice cover and glacial ice loss. Our results imply that future deglaciation of Svalbard fjords will likely increase primary productivity in a "blue" (summer ice-free) scenario; however, the potential for fjords to serve as hotspots of marine organic carbon burial will likely be constrained due to warmer, stratified waters and reduced meltwater-induced supply of critical nutrients.

The most dramatic changes observed of the recent past in response to global warming are the unprecedented reduction in Arctic sea ice extent and enhanced glacial ice loss, which now accounts for over 25% of observed global sea level rise[1]. As a result, climate models project a "blue" (summer ice-free) Arctic Ocean by the mid-21st century[2], with dramatic impacts on marine ecosystems due to increased primary production[3], "Atlantification"[4] and meltwater-induced ocean stratification[5]. The key element of uncertainty in future projections is, however, how the marine ecosystem in a "blue" Arctic will respond to an increasingly warmer future climate. This question of global significance can be addressed by investigating Arctic past "greenhouse" (i.e., warmer-than-present) climate states.

Fjords are among the most productive ecosystems in the Arctic and contain the high-resolution geological archives necessary to understand dynamic changes of marine ecosystems during past "greenhouse" climate states. Today, the fjords of western Svalbard are deglaciating rapidly[6], with a transition from marine- to land-terminating glaciers accelerated by increasing air and water temperature[7], and enhanced ocean stratification[8]. In Kongsfjorden, northwest Svalbard (Fig. 1A–C), contemporary, rapid ecosystem changes are well documented[9,10], with examples highlighting the impact of oceanic and glacial parameters on the development and changes of phytoplankton biomass in the fjord[11–13]. More specifically, increased glacial suspension load can modify phytoplankton biomass and composition, in favour of low biomass and small cell size communities[11], with rates of bacterial degradation exceeding that of new biomass production closer to the glacier compared to outer fjords[14]. Hence, input of glacially-derived meltwater and high suspension load from retreating glaciers deeply affect the ecosystem by limiting light penetration and impact the planktic and benthic activities in Kongsfjorden[15].

Analogous to contemporary research, previous studies in the paleo record have highlighted the impact of Atlantic-derived, warm water intrusions on marine ecosystem changes and instability of marine-terminating glaciers in Kongsfjorden during the Holocene Thermal Maximum (HTM, ~10,000–6000 years ago) (Husum, et al.[16] and references therein); a period of exceptional warmth on Svalbard (ref. 17. Rising water temperatures at the end of the Younger Dryas stadial (~11,600 years ago), similar to the modern temperature increases[18,19], led to increased sediment flux from glacial catchments. The rapid glacial retreat and deglaciation of the fjord resulted in low biological production due to high suspension loads and limited light penetration in surface waters. With the transition to land-terminating glaciers and strong Atlantic water inflow during the HTM,

[1]Geological Survey of Norway, Trondheim, Norway. [2]Department of Geosciences, iC3 – Centre for ice, Cryosphere, Carbon and Climate, UiT The Arctic University of Norway, Tromsø, Norway. [3]Korea Polar Research Institute, Incheon, Republic of Korea. [4]Alfred Wegener Institute, Helmholtz Centre for Polar and Marine Research, Bremerhaven, Germany. [5]Centre for Resilience in Environment, Water and Waste (CREWW), College of Life and Environmental Sciences, University of Exeter, Exeter, UK. [6]Biogeochemistry Research Centre, School of Geography, Earth and Environmental Sciences, University of Plymouth, Plymouth, UK. [7]Department of Earth System Sciences, Yonsei University, Seoul, Republic of Korea. [8]EAWAG, Kastanienbaum, Switzerland. ✉e-mail: jochen.knies@ngu.no

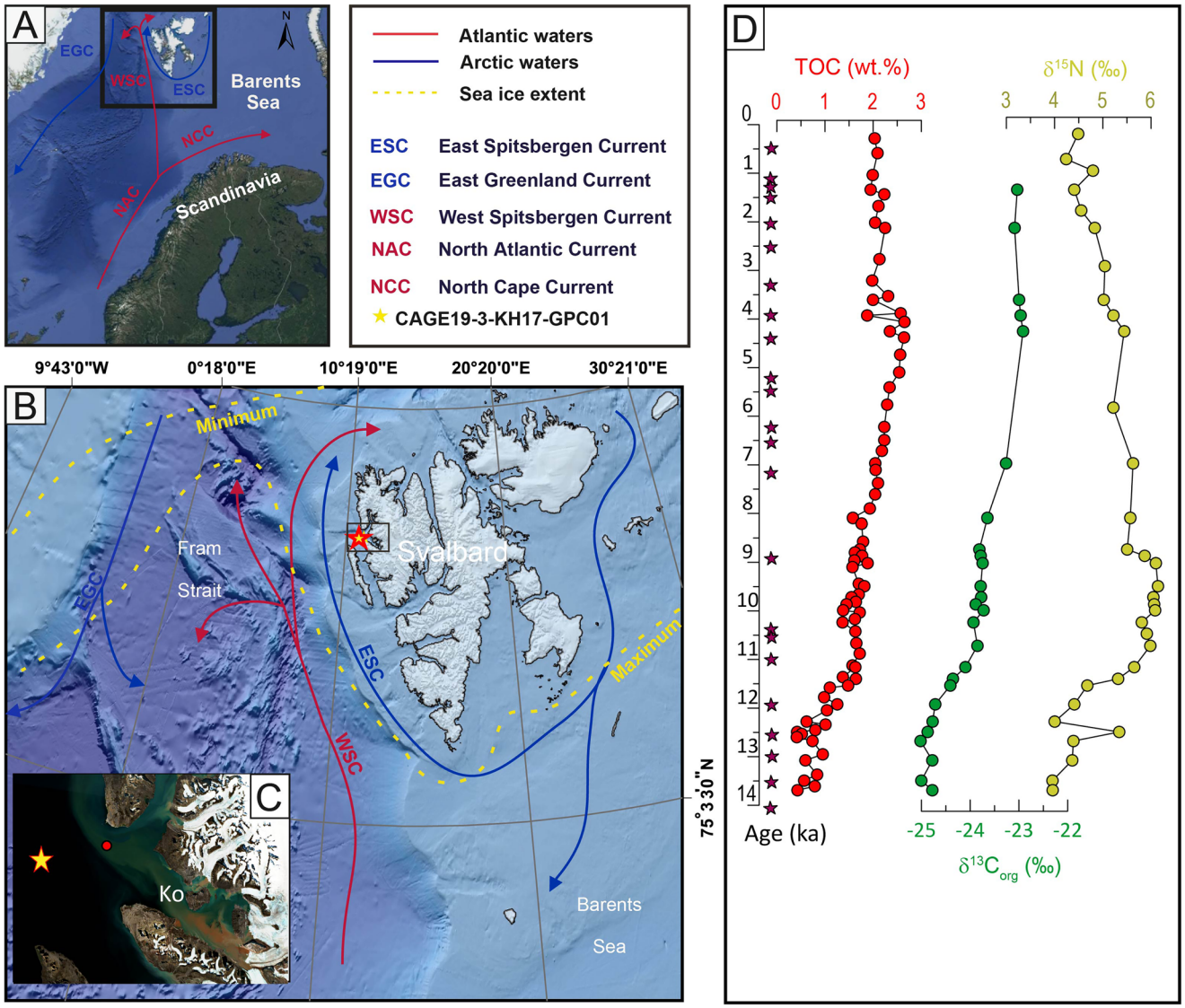

Fig. 1 | Study area. A Nordic seas with main ocean currents. **B** Study area showing the main ocean currents (red and blue arrows) and average minimum sea ice margin for March and maximum sea ice margin for September in the period 1981–2010 (dashed yellow lines) (Data: sea ice extent: NSIDC, 2021). The yellow star indicates the location of KH-17. **C** Satellite image of Kongsfjorden (Ko) (Sentinel 2 L2A, 2020/07/27, available on sentinel-hub.com consulted on 2024/03) and location of KH-17 (yellow star). Red dot indicates station "kb0" in Hegseth and Tverberg[43]. Note the suspension load released from the glacier front during summer melting. For scale, see Supplementary Fig. 4. **D** Bulk geochemical data of KH-17. TOC = Total Organic Carbon (in wt.%), $\delta^{13}C_{org}$ = Stable carbon isotopes (in ‰), $\delta^{15}N$ = Stable nitrogen isotopes (in ‰). Red stars indicate the position of AMS ^{14}C radiocarbon ages (Table S1).

inferred high biological production from foraminiferal assemblages corroborates both high sub-surface and bottom water temperature estimates[16,20]. However, the understanding of the marine ecosystem response to these oceanic and cryosphere perturbations during past warmer-than-present climate states will be more comprehensive if a larger range of phytoplankton groups can be differentiated and is potentially achievable through analysis of source-specific organic geochemical biomarkers preserved in fjord sediments. Such discrimination provides greater insights into the operation of the biological pump and the structure of the food chain in response to changes in cryosphere-carbon feedback during past periods of circum-Arctic ice sheet dynamics.

Several organic biomarkers have now been established for tracing the contribution of different planktonic groups in surface waters to organic carbon (TOC) in sediments. Here we present data from a suite of biomarkers—the highly-branched isoprenoids (HBIs) IP_{25} and HBI III, the sum of C_{37} di- and tri-unsaturated methyl alkenones (i.e., $C_{37:2+3}$), the percentage of a C_{37} tetra-unsaturated methyl alkenone within all alkenones (i.e., $\%C_{37:4}$), and the sterols 24-methylencholesterol, dinosterol and brassicasterol—together with biogenic calcite. These proxy records enable us to trace the contribution of various planktonic groups in surface waters to TOC in sediments, by identifying the production of sea-ice diatoms, diatoms, dinoflagellates, prymnesiophytes, calcareous zooplankton, as well as calcareous benthic grazers, respectively. By showing that the variable concentration maxima of these biomarkers coincide with past ice-ocean interactions in Kongsfjorden over the past 14,000 years, we demonstrate that cryosphere perturbations in response to temperatures changes on Svalbard had enormous consequences for the dominant phytoplankton group in Arctic fjord environments. In a future (warmer-than-present) climate state, we thus predict that enhanced stratification of ocean surface waters and depleted nutrient supply from ice-free terrestrial terrain will lead to reduced transfer of primarily produced TOC to the seafloor in Arctic fjords.

Setting and proxies

The Kongsfjorden system (Fig. 1C) is ca. 20 km long, with a submarine sill separating the fjord from its glacial trough to the west. Water depths vary

between <100 m in the inner part and ~400 m in two basins east and west of the sill (Supplementary Fig. 1). Atlantic and Arctic water masses, as well as glacial meltwater dominate the hydrography (Fig. 1A–C). Warm and saline Atlantic waters (>3 °C, >34.65 psu) via the West Spitsbergen Current entering Kongsfjorden are mixed with cold and fresh Arctic waters (~ −1.5 °C, ~34.5 psu)[21]. The surface layer has a lower salinity than the water column below and is influenced by glacial meltwater and terrestrial runoff. The deepest water has the highest salinity as a result of sea-ice formation and subsequent brine release[22]. However, recent "Atlantification" of this fjord has emerged as result of enhanced advection of Atlantic waters from the West Spitsbergen Current, with a temperature increase of ca. 0.06 °C/year at 85 m water depth from 2010 to 2020[23]. Injection of cold and fresh, subglacial water from marine-terminating glaciers in Kongsfjorden produces upwelling and provides nutrients to the photic zone. However, the elevated suspended sediment loads as seen in Fig. 1C and inferred limited light penetration as well as stratified waters resulting from glacial melting processes may impede enhanced surface productivity, as turbid plumes are predominantly generated by tidewater glaciers when they collapse and melt near the fjord's head[15]. In the Kongsfjorden glacial trough, surface water productivity is controlled by wind-driven upwelling and downwelling associated with off- and on-shore Ekman transport[21]. Phytoplankton dynamics in Kongsfjorden show main biomass production in April–May dominated by diatoms and prymnesiophytes, followed by a low biomass community characterised by dinoflagellates and protozoan grazers during summer[24]. The annual primary production has been estimated to be 35–50 g C m^{-2} in Kongsfjorden[25]. The overall terrestrial TOC contribution remains low (10%) in the outer Kongsfjorden[26,27].

Sediment core CAGE19-3-KH-17-GPC01 (hereafter KH-17) was recovered from the outer Kongsfjorden system (79.026°N, 10.756°E, 325 m water depth) with a Calypso Giant Piston corer (Fig. 1C). Age control over the past 14,000 years is provided by 25 AMS ^{14}C radiocarbon datings (Supplementary Table 1, Supplementary Fig. 2). Sedimentary organic bulk parameters (TOC, $\delta^{13}C_{org}$, $\delta^{15}N$) have been used to infer the dominant organic matter (OM) sources or the relative changes in nutrient utilisation by phytoplankton uptake in surface waters[28]. Biogenic calcite is inferred from high correlation coefficients ($R^2 = > 0.9$, $n = 12$) between XRD-derived calcite (rel. %), XRF calcium (ppm), and calcium carbonate ($CaCO_3$, wt. %) across the record (Supplementary Table 2, Supplementary Fig. 3). Source-specific lipid biomarkers are applied on sedimentary archives for differentiating phytoplankton groups in a changing polar marine ecosystem[29]. Dinosterol is found in many dinoflagellates and was used in this study to indicate dinoflagellate contribution to the sediments[30]. Long-chain C_{37} (di and tri-unsaturated) methyl alkenones are generally used to trace input from prymnesiophytes algae[31], with the relative abundance of the C_{37} tetra-unsaturated compound ($\%C_{37:4}$) as a tracer for sea ice coverage[32]. We also analysed brassicasterol, which is mainly delivered from diatoms during spring[33]. 24-methylenecholesterol is documented in Arctic sea-ice algal communities[34] and is the dominant sterol in marine diatoms of the genus *Thalassiosira*[35]. 24-methylenecholesterol and *Thalassiosira* spores prevailed in northern Norwegian fjords dominated by Arctic waters and seasonal sea ice coverage during the Younger Dryas[28,36,37]. The mono-unsaturated HBI IP_{25} synthesised by certain sea ice diatoms[38] is a common biomarker in Arctic surface sediments underlying seasonal sea ice cover[29], while absent (or very low abundance) in areas that are ice-free or perennial ice covered, year-round. A further tri-unsaturated HBI (generally referred to as HBI III) is used here as a pelagic proxy primarily produced by the diatom *Rhizosolenia setigera*[39] in regions of open water found adjacent to sea ice (i.e., the marginal ice zone (MIZ)) in both polar regions[29]. All data are available in Supplementary Table S3.

Fjord ecosystem response to cryosphere change

High sediment discharge (0.04–0.18 cm/year) (Supplementary Fig. 2) to the outer fjord environment results in the rapid burial of OM in the underlying sediments. The close correspondence of TOC and the bulk $\delta^{13}C_{org}$ isotopic signal (Fig. 1D) may indicate minimal changes in the various proportions of bulk OM due to diagenetic overprint. Instead, the strong variability of $\delta^{13}C_{org}$, and $\delta^{15}N_{tot}$ values suggests a prominent response of the OM composition to climate-induced changes in the sedimentary regime that governs the supply of marine and terrestrial OM (Fig. 1D). Sediment surface studies at the core location report a predominance of marine-produced OM of the carbon supplied to the sediments, most likely linked to single-celled phytoplankton in the photic zone[40,41]. The extremely high sedimentation rates (120 cm ka^{-1} on average) at the coring location in the outer Kongsfjorden support the rapid transfer of the primary-produced and laterally supplied terrestrial OM that retains the original composition of the organic matter during transport and settling. By applying a two-end-member mixing model using paired analyses of $\delta^{13}C_{org}$ and bulk nitrogen signatures in surface sediments around Svalbard[26], it is evident that marine OM dominates the organic fraction during the Holocene (>50%), while terrigenous OM input is significantly elevated (>50%) during the Younger Dryas (Table S3). While we note a significant sedimentary OM contribution from petrogenic sources in the inner part of Kongsfjorden[42], it is likely less important in the outer Kongsfjorden glacial trough[41]. The rapid rise in $\delta^{15}N$ (~2‰) in the aftermath of the Younger Dryas coincides with increased proportions (40–60%) of marine OM (Table S3) and reflects an increased relative nutrient utilisation by phytoplankton in surface waters. The gradual depletion in ^{15}N (lower $\delta^{15}N$) during the Holocene, with gradually lower terrestrial OM input (lower $\delta^{13}C_{org}$ values), implies low utilisation of nutrients by phytoplankton in relatively nitrate-rich surface waters, similar to contemporary nutrient levels at the core location in the outer Kongsfjorden (west of station "Kb0" in Hegseth and Tverberg[43]) (Fig. 1C).

To further distinguish the dominant phytoplankton groups in surface waters to changing climate regimes in Kongsfjorden over the past 14,000 years, we analysed source-specific biomarkers in the sedimentary archive of KH-17 (Fig. 2). A single maximum in IP_{25} alongside a low abundance of other biomarkers during the Younger Dryas (Fig. 2A) document extensive seasonal sea ice coverage and very limited production (Fig. 3A) close to the maximum position of the Younger Dryas moraine separating the Kongsfjorden from its glacial trough (Supplementary Fig. 4)[44]. A boost of nutrients released from the retreating glacial ice front dramatically changed the phytoplankton structure at the end of the Younger Dryas cold period (Fig. 2B–F). Specifically, a considerable increase in absolute concentrations of pelagic HBI III (Fig. 2D), dinosterol (Fig. 2F), brassicasterol (Fig. 2G) and some sympagic biomarkers, suggest a vast revitalisation of largely diatom-driven, primary production due to cryosphere-driven nutrient supply at the end of the Younge Dryas (Fig. 3B), although sea ice was likely still present as indicated by increasing 24-methylenecholesterol concentration and high $\%C_{37:4}$ (Fig. 2B, C). However, the occurrence of at least some sea ice at this time appears inconsistent with the absence (below detection limit) of IP_{25}. In various previous studies from northern Norway[36], western Barents Sea[45], the Olga Basin (Barents Sea)[46] and northern Svalbard[47], the end of the Younger Dryas is characterised by a consistent pairing of lower IP_{25} concentration and elevated HBI III abundance due to marginal sea ice conditions, most commonly found for the central Barents Sea in modern times. Indeed, the same characteristic feature of low IP_{25}/high HBI III has been reported for surface sediments from across the central Barents Sea[45,48]. Since HBI III is elevated in KH-17 at ca. 11–10,000 years ago, at a time when both 24-methylenecholesterol and $\%C_{37:4}$ are also high, it is plausible that the failure to detect IP_{25} is simply due to a detection limit issue or because conditions prevented the colonisation of the IP_{25}-producing diatoms within sea ice during this time.

In some previous studies, IP_{25} has been detected in low concentration in surface sediments from western Svalbard, including several sites proximal to the KH-17 core site[49,50], consistent with low annual sea ice occurrence. In contrast, IP_{25} concentration during the Younger Dryas in several previous studies[36,45,47,51] is always high, typically >15 ng/g sediment. However, IP_{25} concentration in KH-17 only reaches ca. 2 ng/g during the Younger Dryas, despite high sea ice extent, which suggests that sea ice conditions within this fjord setting are not as compatible for colonisation by IP_{25}-producing sea ice diatoms compared to more marine environments, as seen in other Arctic

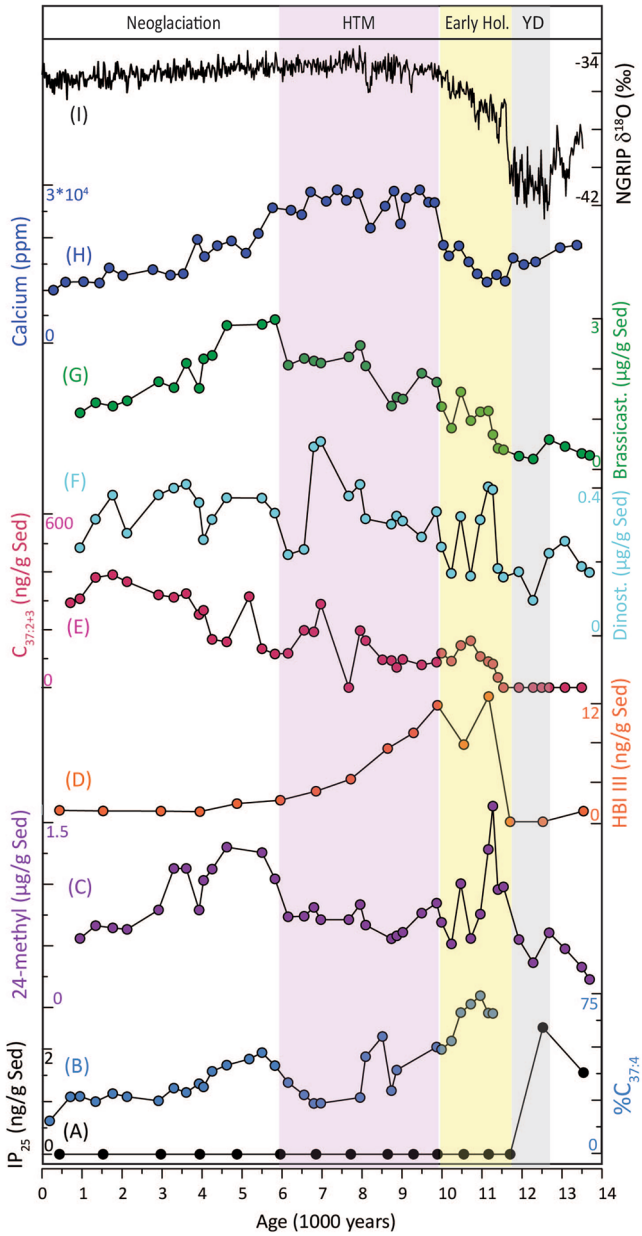

Fig. 2 | Proxy data for Kongsfjorden ecosystem changes. A HBI IP_{25} (ng/g Sed.) **B** Relative abundance (%) of C_{37} tetra-unsaturated methyl alkenone (%$C_{37:4}$) **C** 24-methyl-cholesterol (µg/g Sed.) **D** HBI III (ng/g Sed) **E** C_{37} di and tri-unsaturated methyl alkenones (ng/g Sed.) **F** Dinosterol (µg/g Sed.) **G** Brassicasterol (µg/g Sed.) **H** Calcium (ppm) **I** NGRIP $\delta^{18}O$ (‰)[68].

fjords or regions with higher freshwater input[52–54]. However, a suite of possible scenarios have been presented to explain possible IP_{25} absence in sediments from seasonally sea ice covered regions[29] such that any interpretation of IP_{25} presence is likely more robust than when it is absent[29].

A subsequent decline in the concentrations of 24-methylenecholesterol and HBI III along with a reduction in %$C_{37:4}$ (apart from a short rise in %$C_{37:4}$ between 9000 and 8000 years ago, potentially linked with the 8.2 ka cold event) during the HTM suggests a further depletion of sea ice in the fjord. At the same time, pelagic biomarker concentrations (except for HBI III) remain high, while a characteristic plateau in biogenic calcite implies a rise in calcareous zooplankton and benthos production during the HTM (Figs. 2H, 3C). In a warmer-than-present Arctic climate state, where sea ice is low or absent[20] and an ice-free terrestrial terrain prevails[17], the constantly high $\delta^{15}N$ values together with abundant diatom and dinoflagellate production indicate high nutrient utilisation in a stratified ocean due to significantly warmer surface waters than present[55]. Despite high diatom and dinoflagellate production in surface waters, the prominent rise in calcareous organisms during the HTM suggests high grazing pressure on settling organic biomass (Fig. 3C, D). Plankton dynamics in Kongsfjorden changed again with global cooling during the Neoglaciation (6000–5000 years ago). The intrusion of cold, seasonally sea-ice covered Arctic waters is documented by enhanced %$C_{37:4}$ and concentrations of 24-methylenecholesterol (Fig. B, C). In parallel, nutrient renewal to surface waters from advancing marine-terminating glaciers and deep winter convections in the fjord established the classic spring-bloom paradigm with high diatom production (brassicasterol) (Fig. 2G) as observed today in Kongsfjorden[13,24]. However, a gradual rise of long-chain C_{37} (di-tri-unsaturated) methyl alkenones paralleled by constant brassicasterol and dinosterol concentrations is interpreted to represent the main spring phytoplankton bloom dominated by prymnesiophytes algae (Figs. 2E–G and 3E). Analogous to this scenario are modern observations of seasonal plankton dynamics in Kongsfjorden[12]. In an Atlantic water-dominated regime with little or no sea ice during spring blooms (e.g., spring 2019), bloom-forming diatoms are replaced by prymnesiophytes (e.g., *Phaeocystis*) resulting in gradually less efficient carbon transfer due to increased remineralisation of *Phaeocystis* in surface waters[12].

Past plankton dynamics in warmer-than-present climate states

Future Arctic fjord ecosystems with little or no sea ice and increased Atlantic water inflow will profoundly impact the ocean ecosystem, trophic transfer and eventually carbon sequestration[10,13,43]. The coupled loss of glacial ice will likely lead to a reduced upwelling and stronger water column stratification[56], thus questioning the role of Arctic fjords as hotspots for organic burial in the future[57]. Reduced carbon burial and efficient utilisation of TOC in Kongsfjorden compared to other Arctic fjords (e.g. Hornsund) are indeed interpreted as a result of a gradual change towards an Atlantic water-dominated climate regime[23,58,59], and corroborate inferences from seasonal plankton dynamics in Kongsfjorden that, during periods of stronger Atlantic water influence and less sea ice, the emerging dominance of prymnesiophyte *Phaeocystis* causes a weakening of the biological pump[12]. However, model-based projections on the effects of so-called Atlantification and glacier retreat on fjord circulation, primary and secondary production, and potential shifts in plankton distribution and abundance in an ice-free fjord environment are presently absent[60]. Alternatively, studying the HTM on Svalbard offers the opportunity to understand the sensitivity of ecosystem dynamics through analogue process research from past greenhouse climate states.

Surface waters in western Svalbard fjords were significantly warmer than present during the HTM[55], with a terrestrial ice-free terrain exhibiting an exceptional warmth[17,61]. The consequences of this warming are seen in the stronger grazing pressure of calcareous zooplankton and benthic producers on primarily produced TOC in Kongsfjorden as seen by the high biogenic calcite concentrations during the HTM (Fig. 3C). Despite inferred higher phytoplankton productivity in ice-free waters[10], pelagic biomarker production remains unchanged before, and after the HTM. A likely scenario for Kongsfjorden during the HTM is that surface water stratification due to ocean warming inhibited the nutrient flux from deep waters leading to higher utilisation of available nutrients due to limited phytoplankton production. We propose that, during the HTM, grazing by zooplankton in mixed layer depths likely exceeded any subsequent and associated pelagic-benthic coupling (e.g., via faecal pellet deposition) resulting in low carbon transfer from the photic zone, while high benthic production at the seafloor limited the burial of primarily produced TOC. We support this argument by observing both a distinct plateau of biogenic calcite (Fig. 2H) and the highest fluxes of planktic and benthic foraminifera in Kongsfjorden sediments during the HTM[20]. Moreover, this scenario corroborates modern experiments in Kongsfjorden and the Barents Sea shelf where, with ocean warming and acidification, more OM will be retained in surface waters due to smaller phytoplankton species, increased remineralization, and more intense grazing by zooplankton, more generally[62,63].

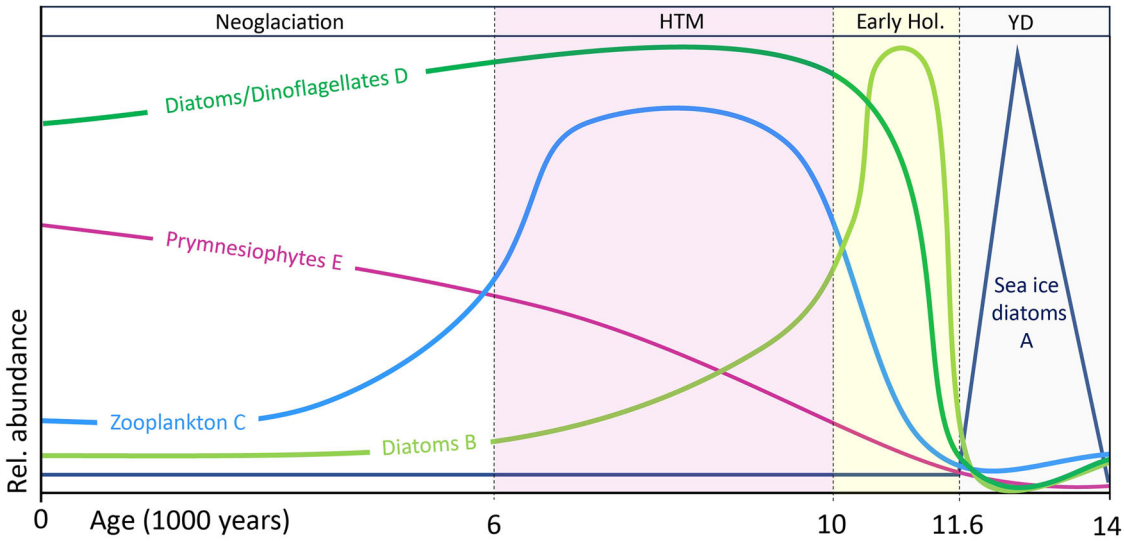

Fig. 3 | Relative changes in phytoplankton groups over the past 14,000 years. Relative changes in phytoplankton groups inferred from the proxy data in Fig. 2 over the past 14,000 years. Colour coding of Holocene Thermal Maximum (HTM), the Early Holocene (Early Hol.) and the Younger Dryas (YD) are the same as in Fig. 2.

We find a coupling of high sedimentation rates (up to 0.18 cm/year) (Supplementary Fig. 2) and an explosion of biological life in surface waters in the aftermath of the Younger Dryas. Such a scenario would have resulted in the rapid transfer of biomass to the seafloor resulting in efficient vertical transport and less recycling, and resembles the well-known modern MIZ conditions in the northern Barents Sea[62] where measured accumulation rates of TOC are more than twice as high as in the ice-free southern Barents Sea[64]. Hence, transfer and storage of primarily produced carbon in Kongsfjorden was more efficient in the proximity of the MIZ together with glacially induced nutrient supply and mineral ballast released from nearby glacier ice. During deglaciation of the Younger Dryas ice sheet on Svalbard, MIZ effects on productivity and carbon transfer would have been further stimulated by proglacial upwelling and nutrient flux to the photic zone of the fjord and differed from conditions during Neoglacial re-advances when sedimentation rates remained significantly lower, and productivity largely controlled by vertical ocean mixing and wind-driven upwelling in the outer Kongsfjorden.

Considering today's abrupt Arctic warming and amplification, our result suggests that fjords remain a hotspot for carbon transfer and storage during a transitional phase from marine to land-terminating glaciers yet will likely lose this efficiency once the fjords experience an ice-free terrestrial terrain in the future.

Methods

Analyses of total carbon and TOC were performed on a bulk and carbonate-free sub-sample using a LECO SC-632 with a standard deviation of ± 0.06 wt %. Carbonate was calculated and confirmed to be largely biogenic calcite by X-ray diffractometry (XRD) and X-ray fluorescence scanning (Supplementary Table 2, Supplementary Fig. 3). Bulk mineral assemblages of dried, homogenised powder (<20 µm particle size) were measured via X-ray diffraction (XRD) using a Bruker D8 Advance diffractometer with Cu Kα radiation and a Lynxeye XE detector at the Geological Survey of Norway, Trondheim. XRD scans were carried out for 3–75° 2θ and a step size of 0.02°. Signal acquisition time was 0.5 s per step. The optical system was equipped with soller slits (2.5°) and fixed divergence (0.6 mm). *X*-ray fluorescence (XRF) core logging was carried out with the Standard MSCL (MSCL-S) core logger (GeoTek Ltd., UK) and an attached DELTA Handheld XRF sensor. The XRF sensor is equipped with a 4-W Rh Tube anode and Si drift detector. Prior to core measurements, the XRF sensor was standardised, and SRM 2710a Montana soil I standard sample[65] was stationary measured for sensor-control purposes. Down core XRF measurements were taken incrementally along the longest axis in the centre of the split core surfaces with 1 cm steps. Two measurements in succession with 40 keV and 10 keV currents and 10 s exposure time each provided spectra covering chemical elements from Mg to Pb, of which only the calcium (Ca) concentrations (ppm) were used for this study.

Stable isotopes of carbon ($\delta^{13}C_{org}$) and nitrogen ($\delta^{15}N$) were measured on Vario PYRO CUBE CN elemental analyser (Elementar, Langenselbold, Germany) connected to an isotope ratio mass spectrometer (IRMS) (IRMS, Isoprime, Manchster, England). For every tenth sample, we ran urea and acetanilide standards with certified values (Schimmelmann, University of Indiana). For the determination of alkenones, 24-methylenecholesterol, brassicasterol, and dinosterol, freeze-dried sediment (~2 g) was extracted in 20 mL of 9:1 Dichloromethane/Methanol (DCM/MeOH) in a microwave reaction system (SolvPro, Anton Paar, Graz, Austria), The microwave was heated to 70 °C over two minutes and held at 70 °C for 5 min[66]. The extracts were saponified (6% KOH), further extracted with hexane, and derivatized with *N,O*-bis(trimethylsilyl) trifluoroacetamide (BSTFA) before injection into a gas chromatography with a flame ionisation detector (GC-FID) (GC-2010 Plus, Shimadzu, Japan). For identification, we used gas chromatography–mass spectrometry (GC–MS) with a QP2020 mass spectrometer (Shimadzu, Japan) and compared the resulting mass spectra to published mass spectra.

HBIs were extracted from ~1 g of freeze-dried and homogenised sediment using 6 ml methanolic KOH (10%) solution following the addition of 100 ng of internal standard (9-octylheptadec-8-ene (9-OHD)). After heating (70 °C; 1 h), samples were extracted with hexane (3 × 2 ml), after which the combined hydrocarbon extract was dried (N_2; 25 °C), then purified using open column chromatography (silica; 60–200 µm, ca. 0.5 g) with HBIs collected using hexane (~6 ml). Partially purified HBI extracts were analysed by gas chromatography-mass spectrometry (GC-MS, Agilent 7890 gas chromatograph) equipped with a HP-5ms fused-silica column coupled to an Agilent 5975 series mass selective detector. IP_{25} and HBI III were identified on the basis of their characteristic retention indices ($RI_{HP\text{-}5ms}$ = 2081 (IP_{25}), 2044 (HBI III)). Individual HBI biomarker concentrations (ng HBI per g dry sediment) were calculated by taking the corresponding GC-MS peak areas, and further normalising using sediment masses, the mass of 9-OHD and individual instrument response factors derived from analysis of purified standards[67].

Data availability

All data needed to evaluate the conclusions in the paper are present in the paper and/or the Supplementary Materials. Links to data are provided below: Supplementary Table S3 Geochemical data of KH-17 - https://doi.org/10.6084/m9.figshare.26641381.v1.

Received: 24 September 2024; Accepted: 27 March 2025;
Published online: 25 April 2025

References

1. Chen, X. Y. et al. The increasing rate of global mean sea-level rise during 1993–2014. *Nat. Clim. Change* **7**, 492–495, https://doi.org/10.1038/nclimate3325 (2017).
2. Intergovernmental Panel on Climate, C. *Climate Change 2021 – The Physical Science Basis: Working Group I Contribution to the Sixth Assessment Report of the Intergovernmental Panel on Climate Change* (Cambridge University Press, 2023).
3. Ardyna, M. & Arrigo, K. R. Phytoplankton dynamics in a changing Arctic Ocean. *Nat. Clim. Change* **10**, 892–903 (2020).
4. Lind, S., Ingvaldsen, R. B. & Furevik, T. Arctic warming hotspot in the northern Barents Sea linked to declining sea-ice import. *Nat. Clim. Change* **8**, 634–639 (2018).
5. Li, W. K. W., McLaughlin, F. A., Lovejoy, C. & Carmack, E. C. Smallest algae thrive as the Arctic ocean freshens. *Science* **326**, 539–539 (2009).
6. Østby, T. I. et al. Diagnosing the decline in climatic mass balance of glaciers in Svalbard over 1957–2014. *Cryosphere* **11**, 191–215 (2017).
7. Isaksen, K. et al. Exceptional warming over the Barents area. *Sci. Rep.* **12**, 9371 (2022).
8. Promińska, A., Cisek, M. & Walczowski, W. Kongsfjorden and Hornsund hydrography – comparative study based on a multiyear survey in fjords of west Spitsbergen. *Oceanologia* **59**, 397–412 (2017).
9. Hop, H. & Wiencke, C. *The Ecosystem of Kongsfjorden, Svalbard* (Springer, 2019).
10. Jørgensen, B. B., Laufer, K., Michaud, A. B. & Wehrmann, L. M. Biogeochemistry and microbiology of high Arctic marine sediment ecosystems—Case study of Svalbard fjords. *Limnol. Oceanogr.* **66**, S273–S292 (2021).
11. Piquet, A. -T. et al. Springtime phytoplankton dynamics in Arctic Krossfjorden and Kongsfjorden (Spitsbergen) as a function of glacier proximity. *Biogeosciences* **11**, 2263–2279 (2014).
12. Assmy, P. et al. Seasonal plankton dynamics in Kongsfjorden during two years of contrasting environmental conditions. *Prog. Oceanogr.* **213**, 102996 (2023).
13. Fang, F. -T. et al. Short-term sedimentary evidence for increasing diatoms in Arctic fjords in a warming world. *Sci. Total Environ.* **951**, 175757 (2024).
14. Sejr, M. K. et al. Glacial meltwater determines the balance between autotrophic and heterotrophic processes in a Greenland fjord. *Proc. Natl. Acad. Sci. USA* **119**, e2207024119 (2022).
15. Meslard, F., Bourrin, F., Many, G. & Kerhervé, P. Suspended particle dynamics and fluxes in an Arctic fjord (Kongsfjorden, Svalbard). *Estuar., Coast. Shelf Sci.* **204**, 212–224 (2018).
16. Husum, K. et al. The marine sedimentary environments of Kongsfjorden, Svalbard: an archive of polar environmental change. *Polar Res*. **29**, 4173–4185 (2019).
17. Farnsworth, W. R. et al. Holocene glacial history of Svalbard: Status, perspectives and challenges. *Earth-Sci. Rev.* **208**, 103249 (2020).
18. Kumar, V., Tiwari, M., Divine, D. V., Moros, M. & Miettinen, A. Arctic climate-Indian monsoon teleconnection during the last millennium revealed through geochemical proxies from an Arctic fjord. *Glob. Planet. Change* **222**, 104075 (2023).
19. Tardif, R. et al. Last Millennium Reanalysis with an expanded proxy database and seasonal proxy modeling. *Climate* **15**, 1251–1273 (2019).
20. Rasmussen, T. L. et al. Spatial and temporal distribution of Holocene temperature maxima in the northern Nordic seas: interplay of Atlantic-, Arctic-and polar water masses. *Quat. Sci. Rev.* **92**, 280–291 (2014).
21. Svendsen, H. et al. The physical environment of Kongsfjorden–Krossfjorden, an Arctic fjord system in Svalbard. *Polar Res.* **21**, 133–166 (2002).
22. Nilsen, F., Cottier, F., Skogseth, R. & Mattsson, S. Fjord–shelf exchanges controlled by ice and brine production: the interannual variation of Atlantic Water in Isfjorden, Svalbard. *Cont. Shelf Res.* **28**, 1838–1853 (2008).
23. De Rovere, F. et al. Water masses variability in inner Kongsfjorden (Svalbard) during 2010–2020. *Front. Mar. Sci.* **9**, 741075 (2022).
24. Hegseth, E. N. et al. In *The Ecosystem of Kongsfjorden, Svalbard* (eds Haakon H & Christian W) 173–227 (Springer Int. Publishing, 2019).
25. Smoła, Z. T. et al. Primary producers and production in Hornsund and Kongsfjorden-Comparison of two Fjord systems. *Polish Polar Res.* **38**, 351–373 (2017).
26. Winkelmann, D. & Knies, J. Recent distribution and accumulation of organic carbon on the continental margin west off Spitsbergen. *Geochem. Geophys. Geosyst.* **6** 2005GC000916 (2005).
27. Krajewska, M., Lubecki, L. & Szymczak-Żyła, M. Sources of sedimentary organic matter in Arctic fjords: Evidence from lipid molecular markers. *Cont. Shelf Res.* **264**, 105053 (2023).
28. Knies, J. Climate-induced changes in sedimentary regimes for organic matter supply on the continental shelf off northern Norway. *Geochim. Cosmochim. Acta* **69**, 4631–4647 (2005).
29. Belt, S. T. Source-specific biomarkers as proxies for Arctic and Antarctic sea ice. *Org. Geochem.* **125**, 277–298 (2018).
30. Boon, J. J. et al. Black Sea sterol—a molecular fossil for dinoflagellate blooms. *Nature* **277**, 125–127 (1979).
31. Brassell, S. C., Eglinton, G., Marlowe, I., Pflaumann, U. & Sarnthein, M. Molecular stratigraphy: a new tool for climatic assessment. *Nature* **320**, 129–133 (1986).
32. Wang, K. J. et al. Group 2i Isochrysidales produce characteristic alkenones reflecting sea ice distribution. *Nat. Commun.* **12**, 15 (2021).
33. Volkman, J. K. A review of sterol markers for marine and terrigenous organic matter. *Org. Geochem.* **9**, 83–99 (1986).
34. Belt, S. T., Brown, T. A., Smik, L., Assmy, P. & Mundy, C. Sterol identification in floating Arctic sea ice algal aggregates and the Antarctic sea ice diatom *Berkeleya adeliensis*. *Org. Geochem.* **118**, 1–3 (2018).
35. Nichols, D. S., Nichols, P. D. & Sullivan, C. W. Fatty acid, sterol and hydrocarbon composition of Antarctic sea ice diatom communities during the spring bloom in McMurdo sound. *Antarct. Sci.* **5**, 271–278 (1993).
36. Cabedo-Sanz, P., Belt, S. T., Knies, J. & Husum, K. Identification of contrasting seasonal sea ice conditions during the Younger Dryas. *Quat. Sci. Rev.* **79**, 74–86 (2013).
37. Oksman, M., Juggins, S., Miettinen, A., Witkowski, A. & Weckström, K. The biogeography and ecology of common diatom species in the northern North Atlantic, and their implications for paleoceanographic reconstructions. *Mar. Micropaleontol.* **148**, 1–28 (2019).
38. Brown, T. A., Belt, S. T., Tatarek, A. & Mundy, C. Source identification of the Arctic sea ice proxy IP_{25}. *Nat. Commun.* **5**, 4197 (2014).
39. Belt, S. T. et al. Identification of C_{25} highly branched isoprenoid (HBI) alkenes in diatoms of the genus *Rhizosolenia* in polar and sub-polar marine phytoplankton. *Org. Geochem.* **110**, 65–72 (2017).
40. Jima, M. et al. Stable isotopic signatures of sediment carbon and nitrogen sources and its relation to benthic meiofaunal distribution in the Arctic Kongsfjord. *Mar. Ecol.* **42**, e12648 (2021).
41. Kim, J. -H. et al. Large ancient organic matter contributions to Arctic marine sediments (Svalbard). *Limnol. Oceanogr.* **56**, 1463–1474 (2011).
42. Kim, D. et al. Large contributions of petrogenic and aged soil-derived organic carbon to Arctic fjord sediments in Svalbard. *Sci. Rep.* **13**, 17935 (2023).

43. Hegseth, E. N. & Tverberg, V. Effect of Atlantic water inflow on timing of the phytoplankton spring bloom in a high Arctic fjord (Kongsfjorden, Svalbard). *J. Mar. Syst.* **113**, 94–105 (2013).
44. Henriksen, M., Alexanderson, H., Landvik, J. Y., Linge, H. & Peterson, G. Dynamics and retreat of the Late Weichselian Kongsfjorden ice stream, NW Svalbard. *Quat. Sci. Rev.* **92**, 235–245 (2014).
45. Belt, S. T. et al. Identification of paleo Arctic winter sea ice limits and the marginal ice zone: optimised biomarker-based reconstructions of late Quaternary Arctic sea ice. *Earth Planet. Sci. Lett.* **431**, 127–139 (2015).
46. Berben, S. M., Husum, K., Navarro-Rodriguez, A., Belt, S. T. & Aagaard-Sørensen, S. Semi-quantitative reconstruction of early to late Holocene spring and summer sea ice conditions in the northern Barents Sea. *J. Quat. Sci.* **32**, 587–603 (2017).
47. Pieńkowski, A. J. et al. Seasonal sea ice persisted through the Holocene Thermal Maximum at 80°N. *Commun. Earth Environ.* **2**, 124 (2021).
48. Köseoğlu, D. et al. Complementary biomarker-based methods for characterising Arctic sea ice conditions: a case study comparison between multivariate analysis and the PIP_{25} index. *Geochim. Cosmochim. Acta* **222**, 406–420 (2018).
49. Müller, J. et al. Towards quantitative sea ice reconstructions in the northern North Atlantic: a combined biomarker and numerical modelling approach. *Earth Planet. Sci. Lett.* **306**, 137–148 (2011).
50. Smik, L. & Belt, S. T. Distributions of the Arctic sea ice biomarker proxy IP_{25} and two phytoplanktonic biomarkers in surface sediments from West Svalbard. *Org. Geochem.* **105**, 39–41 (2017).
51. Müller, J. & Stein, R. High-resolution record of late glacial and deglacial sea ice changes in Fram Strait corroborates ice–ocean interactions during abrupt climate shifts. *Earth Planet. Sci. Lett.* **403**, 446–455 (2014).
52. Xiao, X., Fahl, K. & Stein, R. Biomarker distributions in surface sediments from the Kara and Laptev seas (Arctic Ocean): indicators for organic-carbon sources and sea-ice coverage. *Quat. Sci. Rev.* **79**, 40–52 (2013).
53. Hörner, T., Stein, R., Fahl, K. & Birgel, D. Post-glacial variability of sea ice cover, river run-off and biological production in the western Laptev Sea (Arctic Ocean)–A high-resolution biomarker study. *Quat. Sci. Rev.* **143**, 133–149 (2016).
54. Ribeiro, S. et al. Sea ice and primary production proxies in surface sediments from a High Arctic Greenland fjord: Spatial distribution and implications for palaeoenvironmental studies. *Ambio* **46**, 106–118 (2017).
55. Mangerud, J. & Svendsen, J. I. The holocene thermal maximum around Svalbard, Arctic North Atlantic; molluscs show early and exceptional warmth. *Holocene* **28**, 65–83 (2018).
56. Torsvik, T. et al. Impact of tidewater glacier retreat on the fjord system: modeling present and future circulation in Kongsfjorden, Svalbard. *Estuar., Coast. Shelf Sci.* **220**, 152–165 (2019).
57. Smith, R. W., Bianchi, T. S., Allison, M., Savage, C. & Galy, V. High rates of organic carbon burial in fjord sediments globally. *Nat. Geosci.* **8**, 450–453 (2015).
58. Zaborska, A. et al. Sedimentary organic matter sources, benthic consumption and burial in west Spitsbergen fjords–Signs of maturing of Arctic fjordic systems? *J. Mar. Syst.* **180**, 112–123 (2018).
59. De Rovere, F. et al. Winter intrusions of Atlantic water in Kongsfjorden: Oceanic preconditioning and atmospheric triggering. *J. Geophys. Res. Oceans* **129**, e2023JC020095 (2024).
60. Bischof, K. et al. In *The Ecosystem of Kongsfjorden, Svalbard* (eds Haakon, H. & Christian, W.) 537–562 (Springer Int. Publishing, 2019).
61. van der Bilt, W. G. M., D'Andrea, W. J., Werner, J. P. & Bakke, J. Early holocene temperature oscillations exceed amplitude of observed and projected warming in Svalbard lakes. *Geophys. Res. Lett.* **46**, 14732–14741 (2019).
62. Wassmann, P. et al. Food webs and carbon flux in the Barents Sea. *Prog. Oceanogr.* **71**, 232–287 (2006).
63. Riebesell, U., Gattuso, J. -P., Thingstad, T. & Middelburg, J. Arctic ocean acidification: pelagic ecosystem and biogeochemical responses during a mesocosm study. *Biogeosciences* **10**, 5619–5626 (2013).
64. Faust, J. C. et al. Does Arctic warming reduce preservation of organic matter in Barents Sea sediments? *Philos. Trans. R. Soc. A* **378**, 20190364 (2020).
65. Mackey, E. A. et al. Certification of Three NIST renewal soil standard reference materials for element content: SRM 2709a San Joaquin Soil, SRM 2710a Montana Soil I, and SRM 2711a Montana Soil II. *Natl. Inst. Stand. Technol. Spec. Publ.* **260**, 39 (2010).
66. Randlett, M. E. et al. Biomarkers in L ake V an sediments reveal dry conditions in eastern A natolia during 110.000–10.000 years BP. *Geochem. Geophys. Geosyst.***18**, 571–583 (2017).
67. Belt, S. T. & Smik, L. Analytical inconsistencies in the measurement and reporting of IP_{25}, $IPSO_{25}$ and related biomarkers for paleo sea ice reconstruction: Organic Geochemistry, p. 104989. (Elsevier, 2025).
68. Andersen, K. K. et al. High-resolution record of Northern Hemisphere climate extending into the last interglacial period. *Nature* **431**, 147–151 (2004).

Acknowledgements

This research is a part of iC3: Centre for ice, Cryosphere, Carbon and Climate and was supported by the Research Council of Norway (grant numbers 332635, 333241). No permission is required for the sampling of the studied sediment core. J.K. is supported by the ERC synergy grant "i2B" (grant no 101118519). This study is further supported by the Basic Core Technology Development Programme for the Oceans and the Polar Regions (NRF-2021M1A5A1075512 SIN) from the NRF, funded by MSIT, Republic of Korea. We sincerely thank Serge Robert (EAWAG) for the analytical work.

Author contributions

J.K. developed the main idea and wrote most of the text. B.E., Y.A., K.J., and S.I.N. established the age model. L.S., S.T.B., and C.J.S. supervised the analytical work. All authors discussed the results and commented on the manuscript.

Funding

Open access funding provided by UiT The Arctic University of Norway (incl University Hospital of North Norway).

Competing interests

The authors declare no competing interests.

Additional information

Supplementary information The online version contains supplementary material available at https://doi.org/10.1038/s43247-025-02251-y.

Correspondence and requests for materials should be addressed to Jochen Knies.

Peer review information *Communications Earth & Environment* thanks Józef Wiktor, Zhuoyi Zhu and the other, anonymous, reviewer(s) for their contribution to the peer review of this work. Primary Handling Editors: Shin Sugiyama and Carolina Ortiz Guerrero. A peer review file is available